Materials and Design 46 (2013) 366–371

Contents lists available at SciVerse ScienceDirect

Materials and Design

journal homepage: www.elsevier.com/locate/matdes

Technical Report

Residual stress measurement on AA6061-T6 aluminum alloy friction stir butt welds using contour method

Chuan Liu [a,*], Xiang Yi [b]

[a] Provincial Key Lab of Advanced Welding Technology, Jiangsu University of Science and Technology, ZhenJiang 212003, China
[b] Shanghai Aerospace Equipments Manufacturer, Shanghai 200245, China

ARTICLE INFO

Article history:
Received 20 August 2012
Accepted 20 October 2012
Available online 7 November 2012

ABSTRACT

Residual stress is a crucial factor when assessing the integrity of engineering components and welded assemblies. The internal longitudinal stresses in 4 mm and 8 mm thick AA6061-T6 aluminum alloy friction stir welding (FSW) specimens are measured with contour method. The measuring procedure of the contour method including specimen cutting under clamps with a wire electric discharge machine, precise contour measurement with a coordinate measuring machine, careful data processing and elastic finite element analysis are introduced in detail. Finally, the longitudinal residual stresses throughout the cut plane for the two joints are mapped, and the through-thickness longitudinal stresses of the two FSW joints are also analyzed. Investigated results show that the contour method can be applied to measure the internal residual stress in thin plates with a thickness of 4 mm; the longitudinal stress distribution in the present study is not an apparent M-shaped distribution in the transverse direction; within the weld region, the tensile longitudinal stress in the advancing side is larger than that in the retreating side; the longitudinal stresses are not uniform across the thickness of specimens; the peak tensile longitudinal stresses for both joints reach 168 MPa (amount to 61% of the yield strength of AA6061-T6 alloy at room temperature), and appear at a depth of 62.5% thickness at the edge of the tool shoulder in the advancing side of the weld.

1. Introduction

Friction stir welding (FSW) is a relatively new solid-state joining process and is considered to be the most significant development in metal joining in a decade. This joining technique is energy efficient, environment friendly, and versatile. In particular, it can be used to join high-strength aerospace aluminum alloys and other metallic alloys that are hard to weld by conventional fusion welding [1]. In essence, it relies on the generation of heat through rotational friction at the tool shoulder/material interface, followed by extrusion of a plasticized region around the probe as it moves forward constrained by the shoulder and base plate. A FSW joint consists of various zones involving different microstructures and mechanical properties. The heat affected zone (HAZ) is the most distant from the joint centerline. The thermo-mechanically affected zone (TMAZ) and the weld nugget are highly deformed by the material rotational flow [2].

Like in fusion welding, thermal and mechanical stresses appear during FSW. The presence of residual stresses in welded components is known to have a significant influence on the fatigue behavior and thereby, on the component lifetime. Therefore, the residual stress distribution introduced into components owning to FSW and its effects on the structure performance have been widely studied with the numerical simulation method and experiments [3–7]. With the aid of numerical simulation and experiments, Feng et al. [8] stated that the failure of friction stir weld under tensile load is controlled by the combination of the reduction in strength and the residual stresses in the heat affected zone (HAZ). Based on the experimental survey, Woo and Choo [9] found that the softening behaviors occurs in the wide region of the FSW Al 6061-T6 alloy are clearly represented in the residual stress profiles.

Recently, experimental measurements with slitting method and numerical simulations were carried out by Deplus et al. [10] to investigate the residual stress distribution in aluminum alloy friction stir welds, they found that the magnitude of the residual stresses and the shape of their distribution across the FSW welds are strongly influenced by the alloy type and welding parameters. The investigated results of Xu et al. [11] on 12 mm thick aluminum FSW specimen using hole-drilling method indicated that the residual stress profile on the top surface is conventional M-shape while V-shape on the bottom surface. Their results state that the stress distribution through thickness is not uniformed for 12 mm thick plate. Accordingly, estimating the magnitude and distribution of internal stress in FSW welds and characterizing the effects of the welding conditions are deemed necessary.

* Corresponding author. Tel.: +86 (0) 511 84401184; fax: +86 (0) 511 84407381.
E-mail addresses: mse.chuanliu@gmail.com, chuanliu@just.edu.cn (C. Liu).

0261-3069/$ - see front matter © 2012 Elsevier Ltd. All rights reserved.
http://dx.doi.org/10.1016/j.matdes.2012.10.030

Experimental measurement is a direct method to get the residual stress distribution in FSW welds. Slitting method [10], hole-drilling method [11] and diffraction method [12–14] have been used to determined the residual stress distribution in FSW welds. Recently, nanoindentation had been used to determine the surface residual stress of FSW welds [15].

In addition, the full stress distribution including the through-thickness residual stress has been paid much more attention [16]. However, the full internal residual stress is difficult to measure, especially for thin plates. The contour method is a relatively new destructive technique to measure a full map of residual stress with the advantages of being simple, cost effective and insensitive to microstructural variations [17]. It has been used to measure and map the internal residual stress within various FSW welds, such as a 3.18 mm thick AA2198-T851 FSW weld [18], a friction stir processed magnesium alloy plate with a thickness of 6.5 mm [19] and a 25.4 mm thick dissimilar aluminum alloy FSW joint [20].

In the present paper, the longitudinal residual stress in FSW of AA6061-T6 aluminum alloy plates with 8 mm and 4 mm thicknesses were measured with the contour method, the measuring procedure was introduced in detail and the through-thickness longitudinal residual stress distributions in 8 mm and 4 mm thick FSW welds were also analyzed.

2. Welding experiments

The commercial AA6061-T6 aluminum alloy plates are used in the present work. AA6061-T6 is a heat treatable wrought aluminum alloy, and the nominal chemical composition was Al–1.0Mg–0.6Si–0.3Cu (wt.%). Two butt-welded samples were prepared that one had the dimensions of 250 mm long, 270 mm wide and 8 mm thick, the other was 300 mm long, 206 mm wide and 4 mm thick. The welding parameters for 8 mm thick plates include: 250 mm/min traveling speed; 500 rpm clockwise rotating speed. A conical pin tool was adopted characterized by a shoulder diameter of 20 mm, a pin height of 5.8 mm, a pin maximum diameter of 6 mm and a pin cone angle of 10°. The 4 mm thick plates were welded using the following parameters: 300 mm/min traveling speed, 800 rpm clockwise rotating speed. The conical pin tool was also used with a 10 mm diameter shoulder. The pin was characterized by a pin height of 3.8 mm, a pin maximum diameter equal to 5 mm and a pin cone angle of 10°. The dimensions of the two welded specimens are shown in Fig. 1.

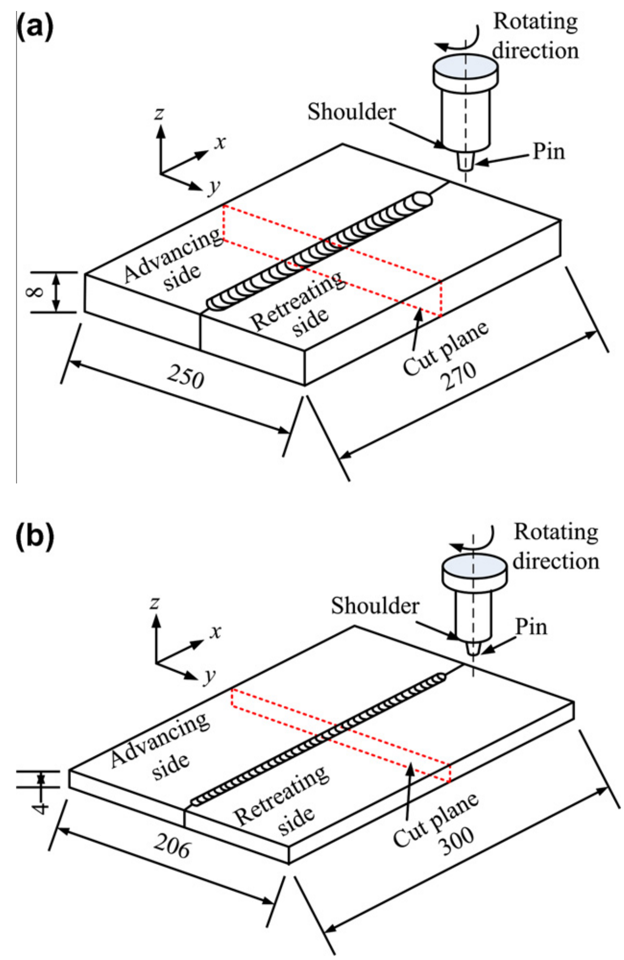

Fig. 1. Dimensions of the two welded specimens (a) 4 mm thick specimen and (b) 8 mm thick specimen.

3. Contour method measurement

The contour method is a newly-invented method to determine the residual stress over a cross-section. The principle behind the contour method is that when a part containing residual stress is cut into halves along a straight line, the newly created free surface will deform as the stresses normal to the surface are released by cutting. The deformations of the cut surface can be measured and used to uniquely determine the initial residual stress acting normal to the cut plane using an elastic finite element model. One of the unique strengths of the contour method is that it provides a full cross-sectional (two dimensional) map of the residual stress component normal to the cross section [17,21]. From Refs. [17,21], main procedures of the contour method include: (1) specimen cutting, (2) contour measurement, (3) data processing, and (4) finite element analysis to determine residual stress that normal to the cut surface.

The cutting step is typically performed using a wire electric discharge machine (EDM). Wire EDM can make a very straight cut, does not remove additional material from previously cut surfaces, does not induce plastic deformation, and results in negligible induced stresses if cutting is performed under the proper conditions [21]. In the present study, the specimens were cut with a SODICK AQ400LS wire EDM machine and securely clamped onto a thick steel backing plate to minimize the amount that the part was able to move as residual stresses were released, as Prime et al. [21] and Dewald et al. [22] did for the stress measurment with contour method.

For specimens with different materials and thickness, the cutting parameters are different. The 0.225 mm/min cutting speed

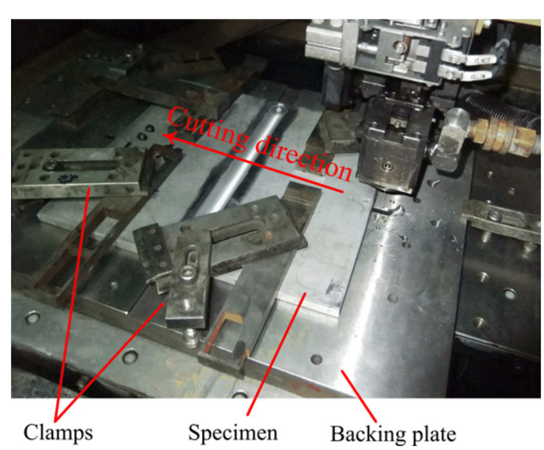

Fig. 2. Cutting process.

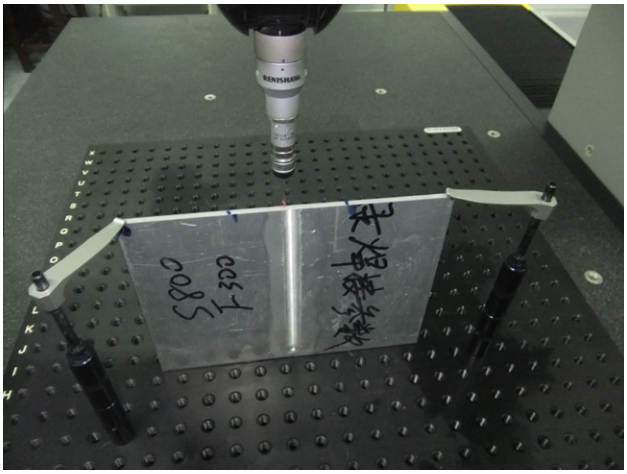

Fig. 3. Contour measurement.

and 0.1 mm diameter brass wire were selected by Prime et al. [20] to perform the cut of a 25.4 mm thick aluminum alloy specimen, 0.25 mm diameter brass wire and about 0.8 mm/min cutting speed were applied to cut a 6 mm thick steel T-joint [23]. Woo employed 0.1 mm diameter brass wire and 0.38 mm/min cutting speed to cut the 6 mm thick magnesium alloy plate [19]. These cutting parameters should be chosen for better precision and a finer surface finish with low likelihood of wire failure, and also for minimizing any recast layer and cutting-induced stresses [17]. In the present study, a 0.2 mm diameter brass wire and 0.5 mm/min cutting speed were used to carried out the cut.

The cut plane is shown in Fig. 1. To prevent any thermal stresses, the weld specimen and fixtures were allowed to come to thermal equilibrium in the water tank before clamping. The clamped specimen was submerged in temperature-controlled deionized water throughout the cutting process. The cutting process is shown in Fig. 2.

The measurement of the cut surfaces in the present study was performed using a HEXAGON GLOBAL coordinate measuring machine (CMM). The point spacing selection is very important for the profile measurement of the cut surface. For the stress measurement in an Alloy 22 weld, both halves of the cut were measured with a point spacing of approximately 0.5 mm in the transverse and depth directions and in the weld region a dense point spacing of 0.25 mm × 0.25 mm was used [22]. In Ref. [24], the measurement points were designed in a fashion with 1 mm increment

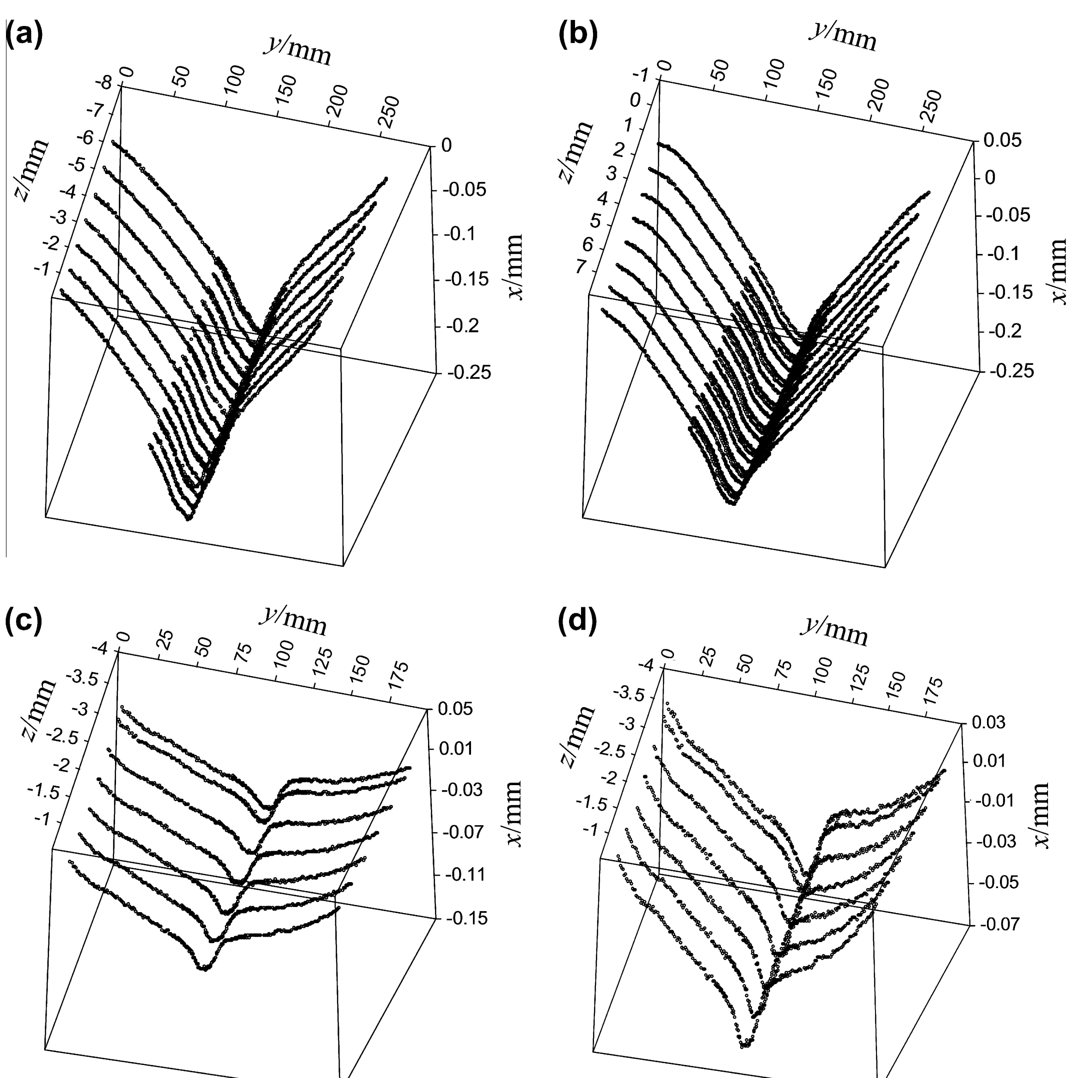

Fig. 4. Raw data of the CMM measurement (a) first cut surface of 8 mm thick specimen, (b) second cut surface of 8 mm thick specimen, (c) first cut surface of 4 mm thick specimen, and (d) second cut surface of 4 mm thick specimen.

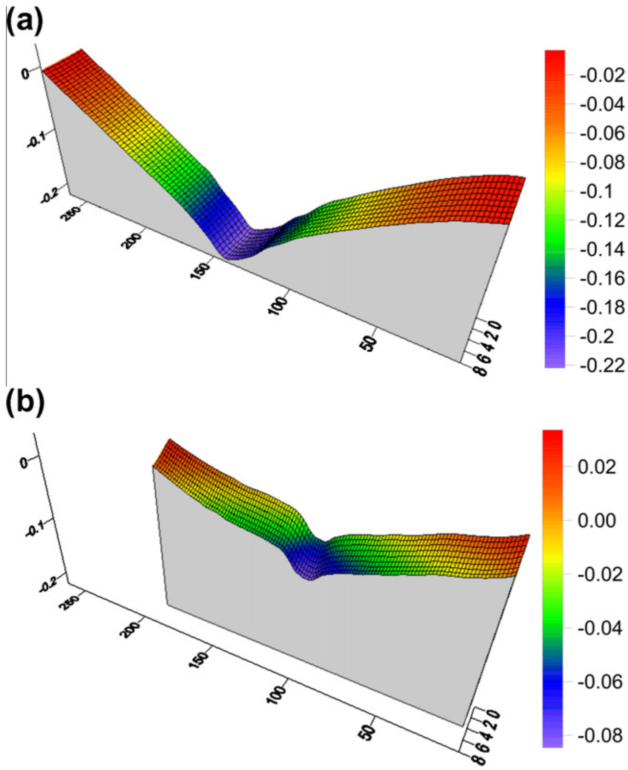

Fig. 5. Smoothed contour of the cut surface (a) 8 mm thick specimen and (b) 4 mm thick specimen.

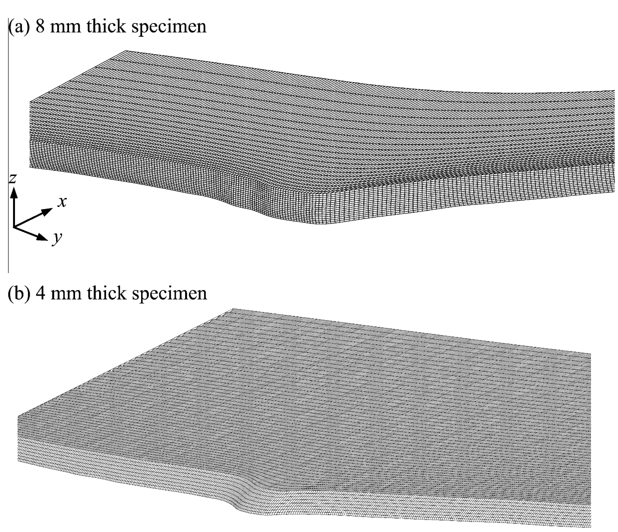

Fig. 6. 3-D finite element models after measured contours have been applied as displacement boundary condition. Displacements magnified by a factor of 300.

along the length and a 0.5 mm increment along the thickness of the cut surface for the stress measurement in a 2024 aluminum alloy variable-polarity plasma-arc (VPPA) weld. For the residual stress measurement of a 316L stainless steel bead-on-plate specimen with contour method, the cut surface was sampled with a measurement point spacing of 0.5 mm × 0.5 mm [25]. In the present study, the point spacing for the profile measurement was chosen according to the above references. For the 8 mm thick specimen, both halves of the cut were measured with a point spacing of approximately 1 mm over the entire cut surface and a region consisting of about 40 mm to either side of the weld center was measured with a point spacing of 0.5 mm to better capture the surface profile in the area of expected stress gradients. For 4 mm thick specimen, the 0.5 mm point spacing was applied over the entire cut surface. The contour measurement is shown in Fig. 3, the measured raw data for 4 mm and 8 mm thick specimens are shown in Fig. 4.

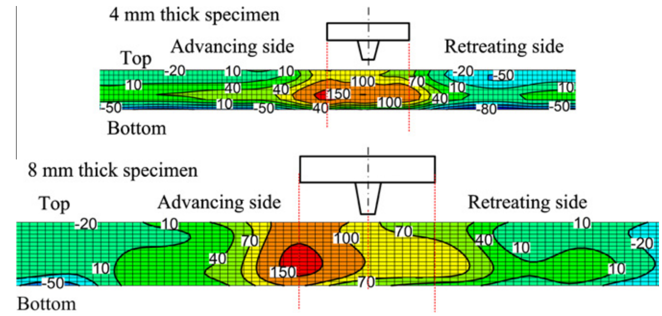

Fig. 7. Map longitudinal stresses on the cut plane (MPa).

After surface profile measurement, the contour measurement points of both cut sides were processed. The most important steps of data analysis are: the alignment of measured data from both cut faces; the removing of noise (bad data) and outliers; the averaging of the two sets of measurements in order to remove shear stress effects and cutting imperfections; and finally fitting smoothly to the cleaned and averaged data. The averaging step is essential as it allows the effect of shear stresses and any imperfections in the

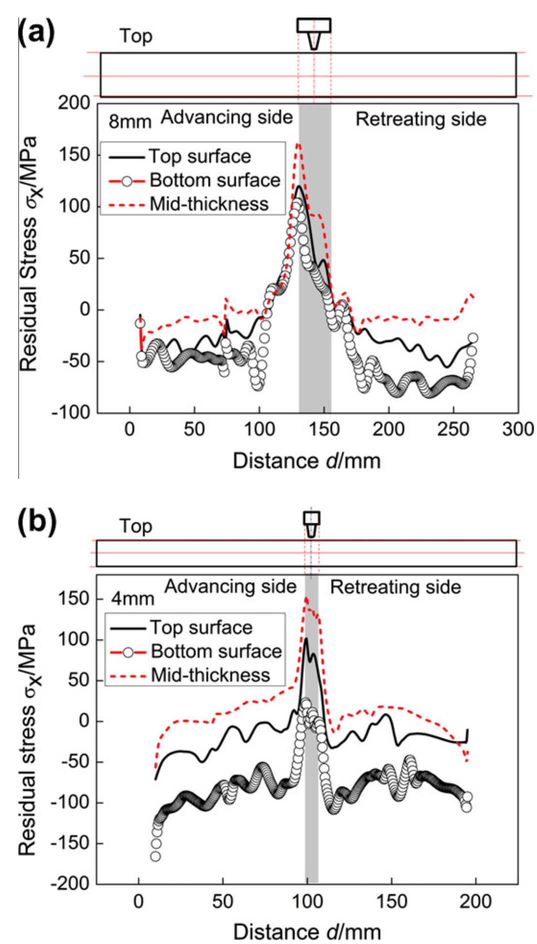

Fig. 8. Residual stress distribution along lines on cut plane (a) 4 mm thick specimen and (b) 8 mm thick specimen.

cut to be removed [17]. The averaged data was smoothed using a cubic spline based algorithm, which is a common algorithm to smoothly fit the contour data in contour method [17,21,26], the final smoothed surfaces are shown in Fig. 5.

The stresses normal to the cut plane were finally inferred by applying the smoothed contour as a boundary condition, but with reversed sign, as a series of displacements to the previous flat cut face of a one-half plate FE model representation of the weld plate geometry. A linear elastic finite element analysis was then undertaken to calculate the corresponding distribution of residual stress. A Young's modulus of 69 GPa and Poisson's ratio of 0.34 were employed [16]. The three-dimensional elastic finite element analysis was performed with the ANSYS software. The mesh was built using the three-dimensional 8-node structural solid elements (solid185 element) with 0.5 mm × 0.5 mm dimensions in the cut plane for the two samples. The entire model was restrained with two corner nodes to prevent rigid body motion, as Prime et al. [21] did. The 3-D finite element models after measured contours have been applied as displacement boundary condition for the two specimens are shown in Fig. 6.

4. Results and discussions

The measured stress with contour method is that normal to the cut surface, therefore, the x-direction stress (longitudinal stress) is measured in the present study.

A map of longitudinal stresses within the weld and its adjacent region from the contour method measurement for 4 mm and 8 mm thick specimens are shown in Fig. 7. From Fig. 7, it can be seen that the longitudinal stress distribution is almost entirely tensile throughout the thickness within the weld region for the two specimens, except that a small compressive stress is present on the bottom surface of the 4 mm thick joint. A transition of stress from tension (weld and near to the weld) to very small stress (away from the weld) is clearly obvious from the contour map, the width of the tensile stress region is larger than that of the shoulder width (width of the TMAZ). It is also clearly observed that the longitudinal residual stress near the advancing side is higher than that near the retreating side for the two joints. The peak tensile stress occurs near the advancing side for both 4 mm and 8 mm thick joints. The contours of the longitudinal stress distribution in the present study are similar to those in the aluminum friction stir butt welds obtained by neutron diffraction [27] and contour method [18,28]. Deplus et al. [10] summarized the residual stress results in aluminum alloy friction stir welds in literature with different measurement methods, they drawn a conclusion that the longitudinal residual stress is tensile in the welding region and compressive in the base material, the maximum longitudinal residual stress is generally found in the HAZ. The conclusion is coincident with the results in the present study. Accordingly, it is can be concluded that the contour method used in the present study can get the full map of the longitudinal stresses and their features in 4 mm and 8 mm thick aluminum alloy FSW specimens.

It can be also seen from Fig. 7 that the longitudinal stress is not uniform through the thickness even for the 4 mm thick weld. To clearly demonstrate the longitudinal stress distribution along the thickness, three lines located on the top surface, the mid-thickness plane and on the bottom surface are selected and the stresses along these lines are compared in Fig. 8a and b for 4 mm and 8 mm thick specimens, respectively.

Since the contour method requires extrapolation of data to the borders of the plate due to measurement restrictions approximately 0.1 mm below the surface, the results near the borders may be exaggerated at some points and should therefore not receive too much attention. Nevertheless good measurement results have been obtained [18]. In addition, the stress distribution trends near the borders can be obtained by the contour method [29]. Therefore, it is believed that the stress variation trend along the thickness can be captured by the contour method measurement.

As shown in Fig. 8, the tensile longitudinal stress are not uniform throughout the thickness, the magnitude of the peak tensile stress at the mid-thickness line (about 163 MPa for 8 mm thick plate, 154 MPa for 4 mm thick plate) is larger than those at the top surface and the bottom surface.

The highest tensile residual stresses along these lines are collected at the edge of the weld in the advancing side. The high residual stresses attained on the advancing side of the weld are associated with the high relative speed developed between the welding tool and the workpiece during processing. High relative speeds during processing lead to the development of higher temperatures in comparison to those attained in the retreating side of the weld [28].

Also seen from Fig. 8, the stress distribution pattern in the present study is not the distinct "M-shaped" distribution which has been found in many literature [2,30]. However, the longitudinal residual stress distribution pattern in the present study is very similar to that in a 12.5 mm thick AA 2195 FSW weld [28]. The difference in the distribution pattern of the residual stresses among the different investigations could be attributed to the different material and parameters used during welding [2,10]. These parameters can affect the residual stresses development and residual distribution pattern during welding.

The stresses are not uniform throughout the thickness as shown in Figs. 7 and 8. To clearly reveal the longitudinal stress variation through thickness, the through-thickness stress distribution at the locations of weldline center, advancing side and retreating side for the two FSW joints are plotted in Fig. 9a and b.

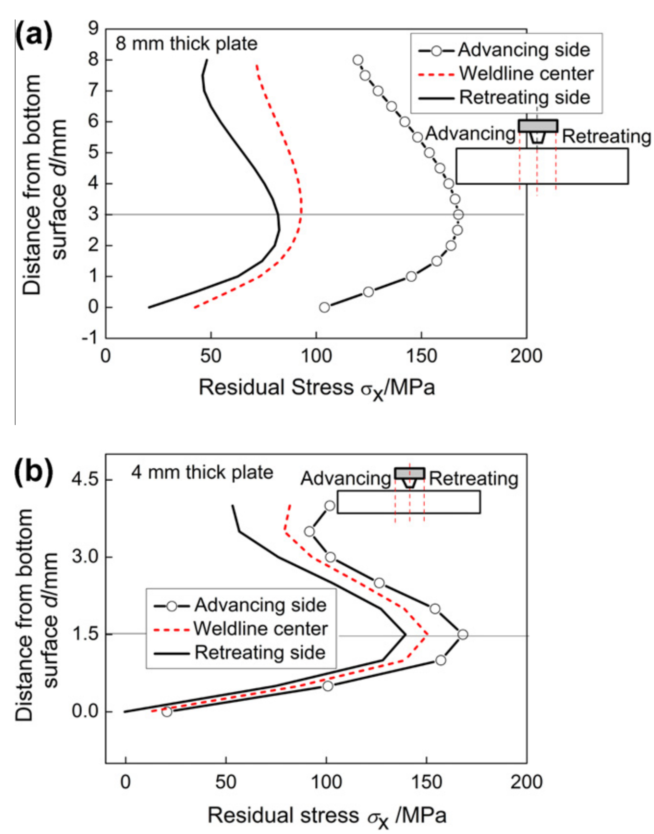

Fig. 9. Through-thickness longitudinal residual stress distribution (a) 8 mm thick specimen and (b) 4 mm thick specimen.

The maximum longitudinal stress is expected at the location of the edge of the weld in the advancing side. From Fig. 9, it can be seen that interior longitudinal stress is larger than those near the top and bottom surface, and the stress near the bottom surface is the smallest one for the given location along the thickness. At the location of the tool shoulder edge in the advancing side of the weld, the longitudinal residual stress reaches a maximum tensile stress (168 MPa for both specimens) at a depth of 62.5% thickness for both FSW joints (5 mm below the top surface for 8 mm thick specimen as shown in Fig. 9a and 2.5 mm below the top surface for 4 mm thick specimen as shown in Fig. 9b) and amounts to 61% of the yield strength of AA6061-T6 alloy, which is 276 MPa at room temperature. The ratio between the maximum tensile residual stress and the base material yield strength in the present study is close to that found by Deplus et al. [10]. They found that in friction stir welding of aluminum alloys, the level of the maximum residual stresses is most of the time significantly lower than the base material yield strength, and it is varying between 40% and 60% of the yield strength in 6082-T6 welds.

5. Conclusion

The internal longitudinal residual stresses in 8 mm and 4 mm thick FSW specimens are measured and mapped using the contour method. The through-thickness longitudinal stresses within the two joints are analyzed. The main conclusions can be summarized as follows:

(1) The contour method can be available to measure the internal residual stress within the FSW joints with 4 mm and 8 mm thickness.
(2) For the FSW joints investigated in the present study, the longitudinal residual stress distribution is not an apparent M-shaped distribution in the transverse direction.
(3) The longitudinal stress at the edge of the tool shoulder in the advancing side of the weld is higher than that in the retreating side for the two joints.
(4) The peak tensile longitudinal stresses for both joints reach 168 MPa and amount to 61% of the yield strength of AA6061-T6 alloy at room temperature, occurring at a depth of 62.5% thickness at the edge of the tool shoulder in the advancing side of the weld.

References

[1] Mishra RS, Ma ZY. Friction stir welding and processing. Mater Sci Eng: R Reports 2005;50(1-2):1–78.
[2] Threadgill PL, Leonard AJ, Shercliff HR, Withers PJ. Friction stir welding of aluminium alloys. Int Mater Rev 2009;54(2):49–93.
[3] Buffa G, Ducato A, Fratini L. Numerical procedure for residual stresses prediction in friction stir welding. Finite Elem Anal Des 2011;47(4):470–6.
[4] Woo W, Feng Z, Wang XL, David SA. Neutron diffraction measurements of residual stresses in friction stir welding: a review. Sci Technol Weld Joi 2011;16(1):23–32.
[5] Pouget G, Reynolds AP. Residual stress and microstructure effects on fatigue crack growth in AA2050 friction stir welds. Int J Fatigue 2008;30(3):463–72.
[6] Fratini L, Macaluso G, Pasta S. Residual stresses and FCP prediction in FSW through a continuous FE model. J Mater Process Technol 2009;209(15–16):5465–74.
[7] Li T, Shi QY, Li HK. Residual stresses simulation for friction stir welded joint. Sci Technol Weld Joi 2007;12(8):664–70.
[8] Feng Z, Wang XL, David SA, Sklad PS. Modelling of residual stresses and property distributions in friction stir welds of aluminium alloy 6061-T6. Sci Technol Weld Joi 2007;12(4):348–56.
[9] Woo W, Choo H. Softening behaviour of friction stir welded Al6061-T6 and Mg AZ31B alloys. Sci Technol Weld Joi 2011;16(3):267–72.
[10] Deplus K, Simar A, Haver WV, Meester BD. Residual stresses in aluminium alloy friction stir welds. Int J Adv Manuf Technol 2011;56(5-8):493–504.
[11] Xu Weifeng, Liu Jinhe, Zhu Hongqiang. Analysis of residual stresses in thick aluminum friction stir welded butt joints. Mater Des 2011;32(4):2000–5.
[12] Staron P, Koçak M, Williams S. Residual stresses in friction stir welded Al sheets. Appl Phys A: Mater Sci Process 2002;74(S1):S1161–2.
[13] Hatamleha O, Dewald A. An investigation of the peening effects on the residual stresses in friction stir welded 2195 and 7075 aluminum alloy joints. J Mater Process Technol 2009;209(10):4822–9.
[14] Lombard H, Hattingh DG, Steuwer A, James MN. Effect of process parameters on the residual stresses in AA5083-H321 friction stir welds. Mater Sci Eng A 2009;501(1–2):119–24.
[15] Charitidis CA, Dragatogiannis DA, Koumoulos EP, Kartsonakis IA. Residual stress and deformation mechanism of friction stir welded aluminum alloys by nanoindentation. Mater Sci Eng A 2012;540:226–34.
[16] Woo W, Choo H, Brown DW, Feng ZL, Liaw PK. Angular distortion and through-thickness residual stress distribution in the friction-stir processed 6061-T6 aluminum alloy. Mater Sci Eng A 2006;437(1):64–9.
[17] Prime MB. Cross-sectional mapping of residual stresses by measuring the surface contour after a cut. J Eng Mater Technol 2001;123(2):162–8.
[18] Richter-Trummer V, Suzano E, Beltrão M, Roos A, dos Santos JF, de Castro PMST. Influence of the FSW clamping force on the final distortion and residual stress field. Mater Sci Eng A 2012;538:81–8.
[19] Woo W, Choo H, Prime MB, Feng Z, Clausen B. Microstructure, texture, and residual stress in a friction stir processed AZ31B magnesium alloy. Acta Mater 2008;56(8):1701–11.
[20] Prime MB, Gnäupel-Herold T, Baumann JA, Lederich RJ, Bowden DM, Sebring RJ. Residual stress measurements in a thick, dissimilar aluminum-alloy friction stir weld. Acta Mater 2006;54(15):4013–21.
[21] Prime MB, Sebring RJ, Edwards JM, Hughes DJ, Webster PJ. Laser surface-contouring and spline data-smoothing for residual stress measurement. Exp Mech 2004;44(2):176–84.
[22] Dewald AT, Rankin JE, Hill MR, Lee MJ, Chen HL. Assessment of tensile residual stress mitigation in alloy 22 welds due to laser peening. J Eng Mater Technol 2004;126(4):465–72.
[23] Murugan N, Narayanan R. Finite element simulation of residual stresses and their measurement by contour method. Mater Des 2009;30(6):2067–71.
[24] Zhang Y, Ganguly S, Edwards L, Fitzpatrick ME. Cross-sectional mapping of residual stresses in a VPPA weld using the contour method. Acta Mater 2004;52(17):5225–32.
[25] Turski M, Edwards L. Residual stress measurement of a 316L stainless steel bead-on-plate specimen utilising the contour method. Int J Press Vess Pip 2009;86(1):126–31.
[26] Hosseinzadh F, Toparli MB, Bouchard PJ. Slitting and contour method residual stress measurements in an edge welded beam. J Press Vess Technol 2012;134(1):011402-1–2-6.
[27] Sutton MA, Reynolds AP, Wang DQ, Hubbard CR. A Study of residual stresses and microstructure in 2024-T3 aluminum friction stir butt welds. J Eng Mater Technol 2002;124(2):215–21.
[28] Hatamleh O, Rivero IV, Swain SE. An investigation of the residual stress characterization and relaxation in peened friction stir welded aluminum–lithium alloy joints. Mater Des 2009;30(9):3367–73.
[29] Liu C, Zhuang D. Internal welding residual stress measurement based on contour method. J Mec Eng 2012;48(8):54–9. in Chinese.
[30] Peel M, Steuwer A, Preuss M, Withers PJ. Microstructure, mechanical properties and residual stresses as a function of welding speed in aluminium AA5083 friction stir welds. Acta Mater 2003;51(16):4791–801.